Results in Physics 31 (2021) 104965

Contents lists available at ScienceDirect

Results in Physics

journal homepage: www.elsevier.com/locate/rinp

Partially coherent UV–VIS light generation in photonic crystal fiber using femtosecond pulses

Miglė Kuliešaitė *, Vygandas Jarutis, Jokūbas Pimpė, Julius Vengelis

Vilnius University, Faculty of Physics, Laser Research Center, Saulėtekio ave. 10, Vilnius 10223, Lithuania

ARTICLE INFO

Keywords:
Photonic crystal fiber
UV–VIS light generation
Femtosecond pulses
Nonlinear optics

ABSTRACT

Light generated in optical fibers due to various nonlinear processes often has a broad spectrum and is commonly considered as a potentially convenient source of seed for tunable wavelength laser systems and many other applications. The nonlinear processes usually considered when discussing this spectrum broadening are coherent.

In this paper we present experimental and theoretical investigation of a partially coherent nonlinear phenomenon occurring at the same time — ultraviolet–visible light (375 nm–500 nm) generation in a short photonic crystal fiber pumped by ~ 110 fs duration and 1028 nm wavelength pulses.

Introduction

Generation of broad spectrum radiation is one of the most important and widely studied topics in nonlinear optics due to a great number of potential applications for broadband laser radiation including spectroscopy [1], frequency metrology [2], optical coherence tomography [3,4], tunable wavelength laser systems [5], etc. In most cases it is termed as continuum generation since the spectrum of radiation expands hundreds or even thousands of times compared to the initial radiation spectrum. A lot of research into continuum generation in a wide variety of media, including photonic crystal fibers (PCFs) [6–22], have been conducted. It is well-known that during spectrum extension in optical fibers many different coherent processes such as self-phase modulation [23], third harmonic and soliton formation [24], four-wave mixing [25], etc. can occur and their interaction shapes the broadened spectrum. Given the appropriate dispersion characteristics, spectrum extension into the UV range can occur in hollow-core PCFs as well [26]. An interesting approach which enables continuum spectrum extension to deep-UV spectral range is use of hollow-core PCF with its core filled with gas (gas-core PCF) [27,28]. By tuning pressure and temperature of the gas, we can actually tune dispersion of such hollow-core gas-filled PCF which in turn yields vacuum-UV (VUV) continuum generation [29]. On the other hand, incoherent UV–VIS light generation is also be observed in fibers: a paper by Amrani et al. [30] reports generation of deep-UV emission fluorescence light using plasma generated in hollow-core PCF from a gas mixture. Moreover, as we describe in this paper, partially coherent processes with peculiar features can also be observed in solid-core photonic crystal fibers without any specific improvements.

In this paper we report investigation of partially coherent UV–VIS light (375 nm–500 nm) generation in a highly nonlinear photonic crystal fiber. We present a theoretical model giving good qualitative explanation of this phenomenon, its partial coherence and other characteristic features. The presented results contribute to a more comprehensive understanding of nonlinear processes occurring in optical fibers.

Experimental setup

The experiment was performed using the setup depicted in Fig. 1a.

The pump source was a mode-locked Yb:KGW laser oscillator "Flint" generating 1028 nm central wavelength (which we will refer to as fundamental harmonic — FH) and 110 fs duration pulses with 76 MHz repetition rate. An optical attenuator, consisting of a half-wave plate mounted on the motorized rotation stage and a Brewster type polarizer, was used to change energy of pump pulses. The laser beam was directed at a pair of prisms, which were used to eliminate pulse chirp induced by the microscope objective, so that transform-limited pump pulses would be observed at the entrance of PCF. A low group velocity dispersion (GVD) telescope and 40x magnification and 0.65 numerical aperture microscope objective were used to focus pump radiation into the PCF. Microscope objective with the input coupling end of PCF was mounted on a Thorlabs Nanomax 300D three-axis translation stage. A polarization-maintaining solid core PCF manufactured by NKT Photonics was used for experiment. A scanning electron microscope (SEM) picture of this PCF cross-section is depicted in Fig. 1b. The PCF

* Corresponding author.
E-mail address: migle.kuliesaite@ff.vu.lt (M. Kuliešaitė).

https://doi.org/10.1016/j.rinp.2021.104965
Received 15 September 2021; Received in revised form 25 October 2021; Accepted 31 October 2021
Available online 12 November 2021

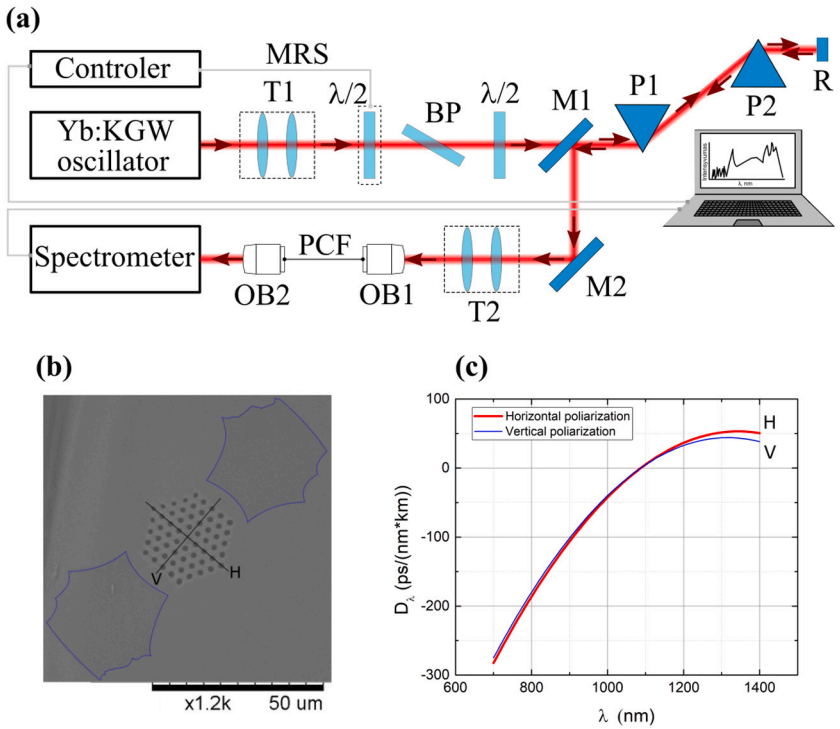

Fig. 1. (a) Experimental setup: $\lambda/2$ — half-wave phase plate; BP — Brewster type polarizer; P1, P2 — prisms; R — retroreflector; M1, M2 — highly reflective mirrors; OB1, OB2 — microscope objectives, PCF — photonic crystal fibe, T1 and T2 — telescopes, MRS — motorized rotation stage. (b) SEM image of the PCF cross-section used in experiments. Blue lines mark extra elements which apply mechanical strain along V axis. (c) The dispersion parameter D for orthogonal polarization modes: V – vertical polarization (thin blue curve) and H – horizontal polarization (thick red curve) of the PCF .

length was 2.6 cm. The core diameter and the pitch of the PCF were 4.8 μm and 3.25 μm respectively. The GVD of this PCF was estimated using a new GVD measurement method based on cross-correlation frequency-resolved optical-gating trace analysis [31]. The estimated GVD curves show that the zero-dispersion wavelength (ZDW) is at 1087.4 nm ± 10 nm for both polarization modes of the PCF (Fig. 1c). We can see that the GVD curves for orthogonal polarization modes are very similar as the difference between the curves becomes visible only in the long-wavelength part (approximately from 1170 nm). In this experiment we used horizontal polarization pump because the results of the measurements were essentially the same for both polarizations. A second identical microscope objective was used to collimate output light coming out of the PCF. Spectra of light coming out of the PCF were measured with an Avantes AvaSpec-ULS2048CL spectrometer with a wavelength range of 200 nm–1100 nm and Ocean Optics NIR Quest 512-2.5 with a wavelength range of 900 nm–2500 nm.

Experimental results

The emission spectra of the fiber were measured for different average powers of the FH, which was from 25 mW to 630 mW at the entrance of the fiber or from ∼ 7 mW to ∼ 190 mW inside the fiber respectively. In Fig. 2a we see that there are three clearly detectable distinct nonlinear processes that take place in the fiber, namely, self modulation of the pump pulse, the generation of the third harmonic (TH) at 343.7 nm and the up converted photo-luminescence (PL) in ultraviolet and visible (UV–VIS) spectral range extended roughly from 375 nm up to 500 nm. It is worth to noting that PL phenomenon differs from other mentioned processes fundamentally in a sense that after light–matter interaction the physical state of material changes as part of energy from the pump beam is delivered to the material and it heats up (in our case up to 60 °C near the entrance of the fiber).

The most striking feature of the UV–VIS light is the modulation of the spectrum which was observed for any power of the FH (see Fig. 2c). This aspect indicates that although UV–VIS light generation is clearly a nonlinear process the modulation of the spectrum most likely is determined by the linear propagation of the light in the fiber and can be used to characterize the coherence properties of emitted light. The dependencies of the average power of the UV–VIS light on the power of the FH is depicted in Fig. 2d. The generation efficiency of UV–VIS light decreases with the increasing power of the FH in PCF. This counter-intuitive result is discussed theoretically in the next section.

Theoretical analysis

The photo-luminescence in the UV–VIS spectral range can be attributed to formation of self-trapped excitons (STE), which are trapped by their interaction with lattice distortion and become attached to lattice sites [32–34]. The threshold of silica glass absorption band is situated approximately at 8.2 eV [33], so at least 7 photons ($\hbar\omega_1$ = 1.2 eV) absorption is needed to excite one free exciton. It is reasonable to assume that free excitons are created along the fiber due to the multi-photon absorption which then decay to STE by emitting the photon in UV–VIS light wavelength range. The spontaneous decay constant of free exciton is about 17 μs [33] while a duration between adjacent pump pulses is just 13 ns. So in order to describe UV–VIS spectrum theoretically we need the model which would be able to take into account spontaneous and stimulated decay of free exciton to STE. To this end we consider the wave equation

$$\frac{\partial^2 \hat{E}(\omega,z)}{\partial z^2} + k^2 \hat{E}(\omega,z) = -\frac{\omega^2}{c^2}\frac{\hat{P}(\omega,z)}{\epsilon_0}, \tag{1}$$

where $k = \omega n(\omega)/c$ is the wavenumber, $n(\omega)$ is the refractive index of the fundamental mode of PCF, $\hat{P}/\epsilon_0$ is the source of UV–VIS light and ϵ_0 is vacuum permittivity. Together with the initial conditions $\hat{E}(\omega,0) = 0$ and $\partial_z \hat{E}(\omega,0) = 0$ the solution of the Eq. (1) is

$$\hat{E}(\omega,z) = \frac{k^2}{n}\int_0^z \sin[k(\zeta - z)]\,\frac{\hat{P}(\omega,\zeta)}{\epsilon_0}\,\mathrm{d}\zeta\,. \tag{2}$$

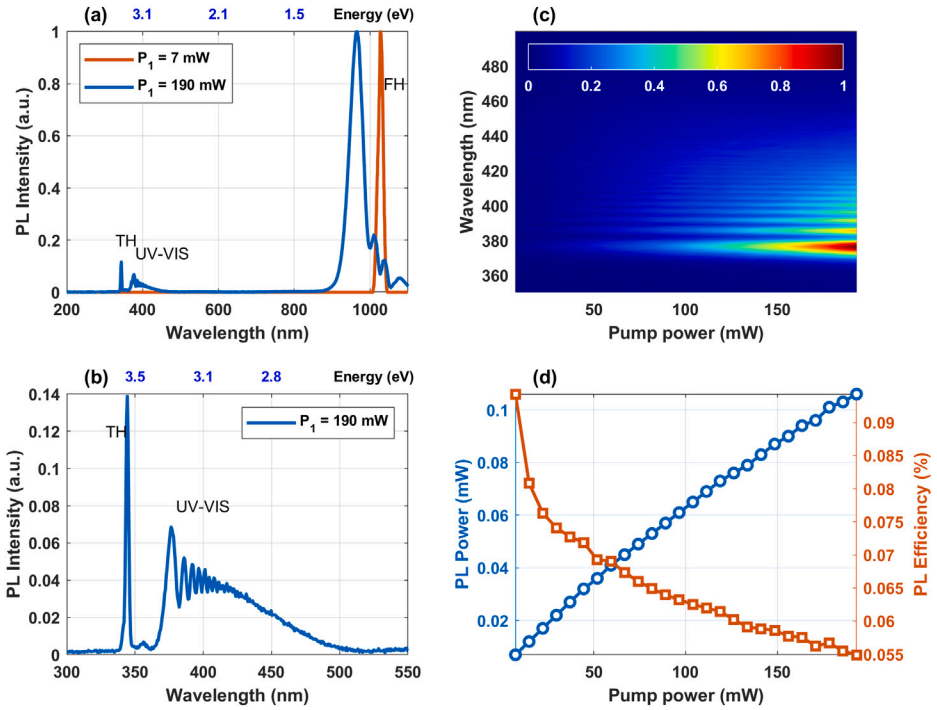

Fig. 2. (a) Typical spectra at the output of PCF for two extreme pump powers — the blue line at 190 mW and the red one for 7 mW. (c) Zoomed in view of spectral range of TH and UV–VIS light. (c) Spectrum modulation of UV–VIS light for different pump power. (d) The average power (blue curve with circle) and the generation efficiency (red curve with square) of UV–VIS light versus average power of the FH. (For interpretation of the references to color in this figure legend, the reader is referred to the web version of this article.)

Assuming that the source of UV–VIS light moves along the fiber with some speed v we model the source by the expression

$$P(t,z)/\varepsilon_0 = [\alpha_N I_1^N]^{1/2} E_0(t - z/v), \tag{3}$$

where I_1 is the intensity of the FH and α_N is N-photon absorption coefficient, so the factor $[\alpha_N I_1^N]^{1/2}$ takes into account N-photon absorption. The $E_0(t - z/v)$ stands for electric field o UV–VIS light emitted in the process of decay of free exciton to self-trapped exciton. For spectrum component we write

$$\frac{\hat{P}(\omega,z)}{\varepsilon_0} = \left[\alpha_N I_1^N\right]^{1/2} e^{iKz + i\phi(\omega,z)}\, \hat{E}_0(\omega), \tag{4}$$

where $K = \omega/v$ and $\phi(\omega,z)$ is the random phase which we introduce here to account exciton–phonon interaction. Considering the simplest plane wave multi-photon absorption model

$$\frac{\partial I_1}{\partial z} = -\alpha_N I_1^N \tag{5}$$

we find

$$I_1(z) = \frac{I_0}{[1 + (N-1)\alpha_N I_0^{N-1} z]^{1/(N-1)}}, \tag{6}$$

where I_0 is the intensity of the FH at the entrance of PCF. Utilizing the fact that the multi-photon absorption is significant only for relatively short length z^* we simplify the whole model by taking $I_1 = I_1(z^*)$ and integrating only up to $z = z^*$. The averaged intensity of the spectral component then is proportional to

$$\langle |\hat{E}(\omega)|^2 \rangle = \alpha_N I_1^N(z^*) \left(\frac{k^2}{n}\right) |\hat{E}_0(\omega)|^2\, F(\omega), \tag{7}$$

where

$$F(\omega) = \int_0^{z^*} \mathrm{d}\zeta\, \sin[k(\zeta - z^*)] \int_0^{z^*} \mathrm{d}\zeta'\, \sin[k(\zeta' - z^*)]\, e^{iK(\zeta - \zeta')} \times \left\langle e^{i\phi(\omega,\zeta) - i\phi(\omega,\zeta')} \right\rangle. \tag{8}$$

The factor $\langle \exp(i\phi(\omega,\zeta) - i\phi(\omega,\zeta')) \rangle$ represents the probability that two waves emitted along the fiber at points ζ and ζ' are summed up coherently. It is modeled in a similar manner as in the model of a light emitted by atoms of gas, i.e.

$$\left\langle e^{i\phi(\zeta) - i\phi(\zeta')} \right\rangle = \exp\left(-\frac{|\zeta - \zeta'|}{l_c(\omega)}\right), \tag{9}$$

where $l_c(\omega)$ is a characteristic coherent length. The larger value of l_c the higher probability of stimulated decay of free exciton to STE. Despite all simplifications the analytical expression of the integral given by the Eq. (8) is quite complicated. However it has the term which is proportional to $\cos[(k - K)z^*]$ and describes the oscillations of the UV–VIS spectrum. By applying the fitting procedure to parameters z^* and v for the most distinguishable peaks of UV–VIS spectrum (see Fig. 3a) we find that $z^* \approx 4$ mm and $v \approx c/1.5240$. Having these values at hand we can estimate the coherent length l_c by considering oscillations amplitudes of UV–VIS spectrum (Fig. 3c). The envelope $|\hat{E}_0(\omega)|^2$ was deduced from experimental spectrum of UV–VIS light by smoothing out all oscillations (Fig. 3b). The simulation results presented in Fig. 3a demonstrate very good agreement between experimental spectrum and its theoretical equivalent. From our model it also follows that stimulated decay of free exciton is more probable in the wavelength range $\sim 375 - -410$ nm where modulation of the spectrum is most observable.

In particular, peaks depicted in Fig. 3(a) correspond to constructive wave interference along the fiber. It is important to stress here that our model does not explain how it happens on an atomic scale. Calculations only demonstrate that if it happens say for peak No. 1, then under the same conditions it happens for other peaks as well. On the atomic scale level one may imagine that electromagnetic oscillations correspond to peaks of UV–VIS light spectrum which induce additional temporal lattice distortions that play the role of trigger for conversion of free exciton to STE.

The generation efficiency of the UV–VIS light is defined as the ratio of a power of generated light to a power of the FH at the entrance of

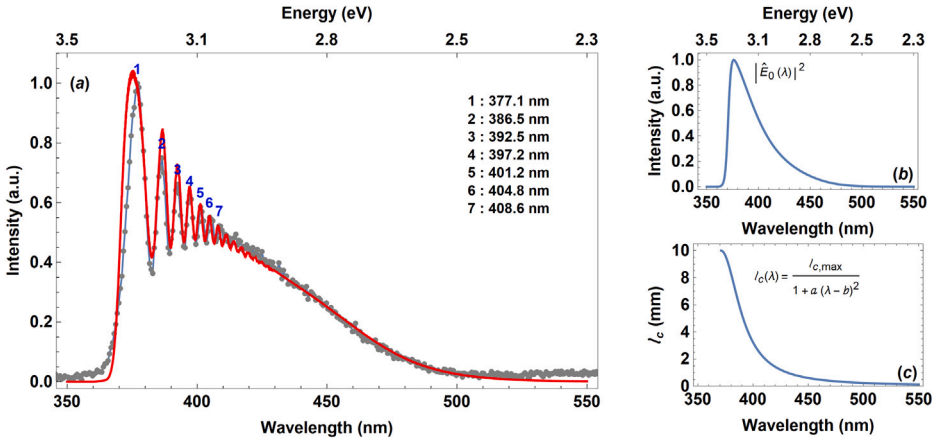

Fig. 3. (a) The spectrum calculated by the (7) is shown as solid (red) curve while the curve with joined circles (gray) represents measured spectrum. Most distinguishable peaks are numbered and their wavelengths are written. (b) The theoretical decay spectrum envelope of free exciton to STE according to our calculations. (c) The empirical function of coherence length $l_c(\lambda)$ of UV–VIS light. Parameters for l_c function: $l_{c,max} = 10$ mm, $a = 50$ nm^{-2}, $b = 371$ nm.

the fiber

$$\eta = \frac{P_{\text{UV–VIS}}}{P_{\text{FH}}} = \frac{\int \varepsilon_0 c \langle |\hat{E}(\omega)|^2 \rangle \frac{d\omega}{2\pi}}{I_0 \tau_p}, \tag{10}$$

where τ_p is the pump pulse duration. Taking into account our simplified model and utilizing Eq. (6) one obtain

$$\eta \propto \frac{I_1^N}{I_0} = \frac{I_0^{N-1}}{[1 + (N-1)\alpha_N I_0^{N-1} z^*]^{N/(N-1)}}. \tag{11}$$

It is not difficult to see that when $(N-1)\alpha_N I_0^{N-1} z^* \geq 1$ the generation efficiency become

$$\eta \propto I_0^{-1} \propto P_{\text{FH}}^{-1}. \tag{12}$$

Although the Eq. (12) does not mimic the generation efficiency of UV–VIS light in full scope, still it demonstrates that at relatively high intensities of the FH the generation efficiency η decreases as pump pulse power P_{FH} increases, in agreement with observed experimental data (Fig. 2d). To model the conversion efficiency of UV–VIS light more accurately it is necessary to take into account other important phenomena such as pump pulse spreading and self-modulation.

Conclusions

During investigation of nonlinear processes in a highly nonlinear photonic crystal fiber when pumping with femtosecond pulses near ZDW, we have determined that there are three clearly detectable and relatively independent nonlinear processes that take place in the fiber, namely, self-modulation of the pump pulse (which eventually leads to continuum generation), generation of the third harmonic and the up-converted photo-luminescence in ultraviolet and visible spectral range.

Our calculations suggest that emission of the UV–VIS light can be attributed to the conversion of a free exciton to a self-trapped exciton. It seems that PL in a fiber in the form of UV–VIS light can interact with free excitons in a coherent way, i.e., the conversion of free exciton to STE for some spectral components of PL is no longer a random process and is tightly related to dispersion characteristics of the fiber. This manifests as spectrum modulation of UV–VIS light. Theoretical analysis has shown that under our experimental conditions excitons are generated most effectively in the first 4 mm of the fiber due to multi-photon absorption. The stimulated decay of free exciton is accompanied by partially coherent UV–VIS light emission in the range ~375 nm – 410 nm which manifests as spectrum modulation. Influence of the partially UV–VIS light generation to other coherent nonlinear processes (which ultimately lead to continuum generation) occurring at the same is not yet clear and will be the subject of further research.

CRediT authorship contribution statement

Miglė Kuliešaitė: Conceptualization, Investigation, Writing – original draft, Visualization. **Vygandas Jarutis:** Software, Formal analysis, Writing – original draft, Visualization. **Jokūbas Pimpė:** Conceptualization, Investigation. **Julius Vengelis:** Methodology, Writing – review & editing.

Declaration of competing interest

The authors declare that they have no known competing financial interests or personal relationships that could have appeared to influence the work reported in this paper.

Acknowledgments

This work has received funding from European Regional Development Fund (project No. 01.2.2-LMT-K-718-03-0004) under grant agreement with the Research Council of Lithuania (LMTLT).

References

[1] Falconieri Mauro, Marrocco Michele, Merla Caterina, Gagliardi Serena, Rondino Flaminia, Ghezelbash Mahsa. Characterization of supercontinuum generation in a photonic crystal fiber for uses in multiplex CARS microspectroscopy. J Raman Spectrosc 2019;50(9):1287–95.
[2] Babushkin I, Tajalli A, Sayinc H, Morgner U, Steinmayer G, Demircan A. Simple route toward efficient frequency conversion for generation of fully coherent supercontinua in the mid-IR and UV range. Light Sci Appl 2017;6:1–8.
[3] Humbert G, Wadsworth W, Leon-Saval S, Knight J, Birks T, Russell PStJ, Lederer M, Kopf D, Wiesauer K, Breuer E, Stifter D. Supercontinuum generation system for optical coherence tomography based on tapered photonic crystal fibre. Opt Express 2006;14(4):1596.
[4] Ghanbari Ashkan, Kashaninia Alireza, Sadr Ali, Saghaei Hamed. Supercontinuum generation for optical coherence tomography using magnesium fluoride photonic crystal fiber. Optik 2017;140:545–54.
[5] Shirakawa A, Sakane I, Takasaka M, Kobayashi T. Sub-5-fs visible pulse generation by pulse-front-matched noncollinear optical parametric amplification. Appl Phys Lett 1999;74(16):2268–70.
[6] Dudley John M, Genty Goëry, Coen Stéphane. Supercontinuum generation in photonic crystal fiber. Rev Modern Phys 2006;78(4):1135–84.
[7] Dudley John M, Provino Laurent, Grossard Nicolas, Maillotte Hervé, Windeler Robert S, Eggleton Benjamin J, Coen Stéphane. Supercontinuum generation in air–silica microstructured fibers with nanosecond and femtosecond pulse pumping. J Opt Soc Amer B 2002;19(4):765.
[8] Lehtonen M, Genty G, Ludvigsen H, Kaivola M. Supercontinuum generation in a highly birefringent microstructured fiber. Appl Phys Lett 2003;82(14):2197–9.
[9] Hilligsøe Karen Marie, Andersen Thomas Vestergaard, Paulsen Henrik Nørgaard, Nielsen Carsten Krogh, Mølmer Klaus, Keiding Søren, Kristiansen Rene, Hansen Kim Per, Larsen Jakob Juul. Supercontinuum generation in a photonic crystal fiber with two zero dispersion wavelengths. Opt. Express 2004;12(6):1045–54.

[10] Buczynski R, Pysz D, Martynkien T, Lorenc D, Kujawa I, Nasilowski T, Berghmans F, Thienpont H, Stepien R. Ultra flat supercontinuum generation in silicate dual core microstructured fiber. Laser Phys Lett 2009;6(8):575–81.
[11] Hooper LE, Mosley PJ, Muir AC, Wadsworth WJ, Knight JC. Coherent supercontinuum generation in photonic crystal fuber with all-normal group velocity dispersion. Opt Express 2011;19(6):4902–7.
[12] Gao Weiqing, Xu Qiang, Li Xue, Zhang Wei, Hu Jigang, Li Yuan, Chen Xiangdong, Yuan Zijun, Liao Meisong, Cheng Tonglei, Xue Xiaojie, Suzuki Takenobu, Ohishi Yasutake. Experimental investigation on supercontinuum generation by single, dual, and triple wavelength pumping in a silica photonic crystal fiber. Appl Opt 2016;55(33):9514.
[13] Vengelis Julius, Jarutis Vygandas, Sirutkaitis Valdas. Extension of supercontinuum spectrum, generated in polarization-maintaining photonic crystal fiber, using chirped femtosecond pulses. Opt Eng 2018;57(01):1.
[14] Pipinyte Ieva, Vengelis Julius, Jarutis Vygandas, Vengris Mikas, Grigonis Rimantas, Sirutkaitis Valdas. Investigation of continuum generation in the non-zero dispersion-shifted fiber pumped by femtosecond nanojoule pulses in 1450-1800 nm spectral range. Results Phys 2020;17:103064.
[15] Van Lanh Chu, Hoang Van Thuy, Long Van Cao, Borzycki Krzysztof, Xuan Khoa Dinh, Quoc Vu Tran, Trippenbach Marek, Buczyński Ryszard, Pniewski Jacek. Supercontinuum generation in photonic crystal fibers infiltrated with nitrobenzene. Laser Phys 2020;30(3).
[16] Le Hieu Van, Hoang Van Thuy, Nguyen Hue Thi, Long Van Cao, Buczyński Ryszard, Kasztelanic Rafał. Supercontinuum generation in photonic crystal fibers infiltrated with tetrachloroethylene. Opt Quantum Electron 2021;53(187).
[17] Dudley John, Gu Xun, Xu Lin, Kimmel Mark, Zeek Erik, O'Shea Patrick, Trebino Rick, Coen Stephane, Windeler Robert. Cross-correlation frequency resolved optical gating analysis of broadband continuum generation in photonic crystal fiber: simulations and experiments. Opt Express 2002;10(21):1215–21.
[18] Tartara L, Cristiani I, Degiorgio V. Blue light and infrared continuum generation by soliton fission in a microstructured fiber. Appl Phys B 2003;77(2–3):307–11.
[19] Efimov Anatoly, Taylor AJ, Russell PStJ. Time-spectrally-resolved ultrafast nonlinear dynamics in small-core photonic crystal fibers: Experiment and modelling. Opt Express 2004;12(26):6498–507.
[20] Cristiani Ilaria, Tediosi Riccardo, Tartara Luca, Degiorgio Vittorio. Dispersive wave generation by solitons in microstructured optical fibers. Opt Express 2004;12(1):124–35.
[21] Gorbach AV, Skryabin DV, Stone JM, Knight JC. Four-wave mixing of solitons with radiation and quasi-nondispersive wave packets at the short-wavelength edge of a supercontinuum. Opt Express 2006;14(21):9854–63.
[22] Marest T, Mas Arabí C, Conforti M, Mussot A, Milián C, Skryabin DV, Kudlinski A. Emission of dispersive waves from a train of dark solitons in optical fibers. Opt Lett 2016;41(11):2454.
[23] Stolen RH, Lin Chinlon. Self-phase-modulation in silica optical fibers. Phys Rev A 1978;17(4):1448–54.
[24] Serebryannikov Evgenii E, Fedotov Andrei B, Zheltikov Aleksei M, Ivanov Anatoly A, Alfimov Mikhail V, Beloglazov Valentin I, Skibina Nina B, Skryabin Dmitry V, Yulin Aleksei V, Knight Jonathan C. Third-harmonic generation by raman-shifted solitons in a photonic-crystal fiber. J Opt Soc Am B 23(9):1975–80.
[25] Coen Stephane, Chau Alvin Hing Lun, Leonhardt Rainer, Harvey John D, Knight Jonathan C, Wadsworth William J, Russell Philip StJ. Supercontinuum generation by stimulated raman scattering and parametric four-wave mixing in photonic crystal fibers. J Opt Soc Amer B 2002;19(4):753–64.
[26] Price JHV, Monro TM, Furusawa K, Belardi W, Baggett JC, Coyle S, Netti C, Baumberg JJ, Paschotta R, Richardson DJ. UV generation in a pure-silica holey fiber. Appl Phys B 2003;77(2–3):291–8.
[27] Joly NY, Nold J, Chang W, Hölzer P, Nazarkin A, Wong GKL, Biancalana F, St J. Russell P. Bright spatially coherent wavelength-tunable deep-UV laser source using an ar-filled photonic crystal fiber. Phys Rev Lett 2011;106(20):1–4.
[28] Belli Federico, Abdolvand Amir, Travers John C, Russell Philip StJ. Highly efficient deep UV generation by four-wave mixing in gas-filled hollow-core photonic crystal fiber. Opt Lett 2019;44(22):5509.
[29] Ermolov A, Mak KF, Frosz MH, Travers JC, Russell PStJ. Supercontinuum generation in the vacuum ultraviolet through dispersive-wave and soliton-plasma interaction in a noble-gas-filled hollow-core photonic crystal fiber. Phys Rev A 2015;92:33821–7.
[30] Amrani F, Delahaye F, Debord B, Alves LL, Gerome F, Benabid F. Gas mixture for deep-uv plasma emission in a hollow-core photonic crystal fiber. Opt Lett 2017;42(17):3363–6.
[31] Vengelis Julius, Jarutis Vygandas, Sirutkaitis Valdas. Estimation of photonic crystal fiber dispersion by means of supercontinuum generation. Opt Lett 2017;42(9):1844–7.
[32] Trukhin Anatoly N. Excitons in sio_2: a review. J Non-Cryst Solids 1992;(149):32–45.
[33] Trukhin Anatoly, Smits Krisjanis, Chikvaidze George. Luminescence of silicon dioxide – silica glass, α-quartz and stishovite. Cent Eur J Phys 2011;9(4):1106–13.
[34] Paleari Alberto, Meinardi Francesco, Brovelli Sergio, Lorenzi Roberto. Competition between green self-trapped-exciton and red non-bridging-oxygen emissions in sio_2 under interband excitation. Commun Phys 2018;(67):1–12.